

Estimating the Parameters of the Waxman Random Graph

Matthew Roughan

ARC Centre of Excellence for Mathematical & Statistical Frontiers, School of Mathematical Sciences, University of Adelaide, Australia.

Jonathan Tuke

School of Mathematical Sciences, University of Adelaide, Australia.

Eric Parsonage

School of Mathematical Sciences, University of Adelaide, Australia.

Summary. The Waxman random graph is a generalisation of the simple Erdős-Rényi or Gilbert random graph. It is useful for modelling physical networks where the increased cost of longer links means they are less likely to be built, and thus less numerous than shorter links. The model has been in continuous use for over two decades with many attempts to select parameters which match real networks. In most the parameters have been arbitrarily selected, but there are a few cases where they have been calculated using a formal estimator. However, the performance of the estimator was not evaluated in any of these cases. This paper presents both the first evaluation of formal estimators for the parameters of these graphs, and a new Maximum Likelihood Estimator with $O(n)$ computational time complexity that requires only link lengths as input.

1. Introduction

The study of random graphs provides insight into the formation of real networks and methods to synthesise test networks for use in simulations. Early research was dominated by the study of Gilbert-Erdős-Rényi (GER) random graphs ([Gilbert, 1959](#); [Erdős and Rényi, 1960](#)), which link two vertices independently with a fixed probability, and hence select particular graphs (with a fixed numbers of nodes) all with equal probability. Due partly to its mathematical tractability this model was studied for many years despite clear limitations in its applicability to real networks.

Random graphs explicitly incorporating geometry became popular with the introduction of the Waxman random graph ([Waxman, 1988](#)), proposed as an alternative to the GER random graph as a more realistic setting for testing networking algorithms. The Waxman graph has subsequently been used in applications as wide-ranging as computer networks, transportation and biology (Waxman's original paper is listed by Google Scholar as having been cited around 3000 times). Moreover, the model has been reinvented at least once so not all use cases can be traced back to this paper.

The GER random graph links every pair of vertices independently with a fixed probability, whereas the Waxman graph reflects that in real networks longer links are often more costly or difficult to construct, and their existence therefore less likely. It links nodes i and j with a probability given by a function of the distance d_{ij} between them.

The form chosen by Waxman was the negative exponential*, *i.e.*,

$$p(d_{ij}) = q e^{-s d_{ij}}, \quad (1)$$

for parameters $q, s \geq 0$. A Waxman random graph is generated by randomly choosing a set of points in a section of the plane (usually the unit square), and then linking these points independently according to the distance between them and (1).

Despite frequent use of the Waxman graph there is no formal literature on how to estimate the parameters (q, s) from a given graph, or set of graphs. In most works the parameter values have been chosen arbitrarily with the authors giving little or no justification for the values used. In many cases authors use the parameter values given in earlier works without regard for their origin or applicability. A few works use more careful estimates, but do not evaluate the estimator performance. They simply apply estimates and report results.

This paper presents the first work of which we are aware on the formal estimation of the parameters of the Waxman graph. As part of our investigation we explain many properties of the Waxman graph and its likelihood function, and derive:

- its average node degree, expected number of edges, and average edge length;
- asymptotic expressions for these for large s ;
- the Kullback-Leibler divergence between Waxman graphs and the GER graph;
- minimal sufficient statistics for the model and hence a MLE for the model parameters.

We present the Maximum Likelihood Estimator (MLE) under the assumption of independence between links, and demonstrate that its performance is close to the Cramér-Rao lower bound. We also compare the MLE to other existing approaches and show its advantages in:

- accuracy;
- computational time complexity (by suitable sampling of the existing link lengths $O(n)$ can always be achieved);
- minimal input (using only the lengths of links which exist or a sufficiently large sample of such links).

Finally we use the MLE to estimate the distance dependence of three real networks, using one biological and two Internet datasets.

2. Background and Related Work

A graph (or network) consists of a set of n vertices (synonymously referred to as nodes) which without loss of generality we label $\mathcal{V} = \{1, 2, \dots, n\}$, and a set of edges (or links)

*Note that our parameterisation differs from that in much of the literature, for reasons to be explained in the following sections.

$\mathcal{E} \subset \mathcal{V} \times \mathcal{V}$. We denote the number of edges by $e = |\mathcal{E}|$. Here we are primarily concerned with undirected graphs, though much work on random graphs is easily generalised to directed graphs.

Two nodes i and j are *adjacent* or *neighbours* if $(i, j) \in \mathcal{E}$. They are *connected* if a path $i = n_1 - n_2 - \dots - n_k = j$ exists, where $(n_l, n_{l+1}) \in \mathcal{E}$, and the graph is connected if all pairs of nodes (i, j) are connected.

The GER random graph $G_{n,p}$ of n vertices is constructed by assigning independently and with a fixed probability each tuple of nodes (i, j) to be in \mathcal{E} . The Waxman random graph generalises this by making the probability of each tuple of nodes an edge dependent on a function p of the distance between the two nodes[†].

While the Waxman graph was originally defined using Euclidean distances on a rectangle or straight line with points on an integer grid, and most subsequent work has considered graphs defined with points randomly placed in the unit square, there is no impediment to choosing points in an arbitrary convex region[‡] with an arbitrary distance metric. Hence, we define a Waxman graph by placing n nodes uniformly at random within some defined region R of a metric space Ω with a distance metric $d(x, y)$ and each pair of nodes is made adjacent independently with probability given by (1).

This differs from Waxman's original parameterisation § (Waxman, 1988)

$$p(d_{ij}) = \beta e^{-d_{ij}/L\alpha} \quad (2)$$

for parameters $\alpha, \beta > 0$, where L is the greatest distance possible between any two points in the region of interest. The advantage of Waxman's parameterisation is that α is a dimensionless constant. Unfortunately, previous authors have confused this notation by reversing the roles of α and β with almost equal regularity, to the point where parameters chosen in one paper have been reversed in another purporting to compare results. Hence, we provide an alternate parameterisation (1) chosen with the estimation problem in mind. We deliberately avoid a dimensionless parameter because real estimates naturally have units and it has been common in the literature to assume incorrectly that use of such a parameter removes dependence on the region shape.

The parameter s determines how dependent links are on distance. Larger s decreases the likelihood of long links.

The use of β in past works on the Waxman graphs has allowed for $\beta > 1$, at which point the function (2) must be truncated, creating a corner in the deterrence function shape. This is undesirable from the point of view of parametric estimation, so we restrict

[†]Some examples of use of the Waxman graph include (Waxman, 1988; Thomas and Zegura, 1994; Zegura et al., 1996, 1997; Doar and Leslie, 1993; Wei and Estrin, 1994; Salama et al., 1997; Verma et al., 1998; Matta and Guo, 1999; Shaikh et al., 1999; Fortz and Thorup, 2004; Neve and Mieghem, 2000; Rastogi et al., 2001; Wu et al., 2000; Guo and Matta, 2003; Kuipers, 2004; Kaiser and Hilgetag, 2004b,a; Gunduz et al., 2004; Carzaniga et al., 2004; Lua et al., 2005; Holzer et al., 2005; Wang et al., 2005; Ahuja et al., 2009; Huang et al., 2007; Malladi et al., 2007; Tran and Pham, 2009; Fang et al., 2011a,b; Costa et al., 2010; Janssen, 2010; Davis et al., 2014).

[‡]Convexity is not strictly required, except where there is the notion that the links are physical, and must themselves lie in the region of interest.

§Although users of the Waxman model commonly state that $\alpha \in (0, 1]$ there is no reason it should not take arbitrary positive values.

$q \in (0, 1]$. In this case q is a thinning of the edges, and we shall see that this allows decoupling of estimation of the two parameters.

There are many variants of the Waxman graph through modifications of the distance deterrence function, for instance [Zegura et al. \(1997\)](#) proposed $p(d; \beta) = \beta \exp(-d/(L - d))$. One of the more interesting variants, which we refer to here as the DASTB (Davis-Abbasi-Shah-Telfer-Begon) graph ([Davis et al., 2014](#)), takes Waxman-like rates for contacts between the agents represented by vertices in the graph, and then considers an edge to exist if at least one contact is made. The number of contacts is assumed to have Poisson distribution with parameter k_{ij} given by the Waxman function (1), and then the probability of at least one contact is $p_{ij}(d) = 1 - \exp(-k_{ij})$. We do not formally consider this model here (though we do adapt their estimation approach) except to note that for sparse networks, the low probability of contact means that the two ensembles of random graphs are similar.

Properties such as connectivity and path lengths in Waxman graphs have been studied in several works ([Thomas and Zegura, 1994](#); [Zegura et al., 1996, 1997](#); [Van Mieghem, 2001](#); [M.Naldi, 2005](#)). However, few have considered the estimation of parameters. Indeed, some of the earlier works compared graphs merely by visual inspection.

The first work we are aware of which attempted to estimate the parameters of a Waxman graph from real data is that of [Lakhina et al. \(2002\)](#). Using a large set of real Internet and geographic data the authors found that an exponential distance-based probability was reasonable. The authors conducted the study with some care, comparing two sets of data and finding consistent results by using a log-linear regression of the link distance function against the link distances. However they made no effort to consider the efficiency or accuracy of their estimator.

Estimation has also been used on the DASTB model ([Davis et al., 2014](#)) by determining the parameters of a binary Generalised Linear Model (GLM). We can adapt this approach to the almost equivalent Waxman graphs by considering that links are the binary outcomes of a treatment which is functionally dependent on link distances through the distance deterrence function, then use a GLM to estimate the parameters.

[Davis et al. \(2014\)](#) showed, using their parameter estimations and Akaike’s Information Criterion corrected for small sample sizes (AICc), that the DASTB graph was a better model for their data than the GER (and provided further comparisons against more complex models), and showed a correlation between s and the population density. This has implications for pathogen persistence in wildlife because density has often been considered a critical parameter of disease transmission. However, if contact over longer distances increases in lower-density populations then pathogen persistence may not be so sensitive to host density, as dense populations do not mix so freely.

The underlying assumption of [Lakhina et al. \(2002\)](#) and [Davis et al. \(2014\)](#) is that *all* of the distances are known, even for links that do not exist. This is possible if all node locations are known, but in practice it is sometimes easier to measure the length of a link that exists – say by probing it – than to estimate the length of a hypothetical link. Consider also graphs for which the “distance” is not a physical quantity, but rather a cost or an administratively configured link-weight, for instance in computer network routing protocols such as OSPF link weights can be the output of an optimisation ([Fortz and Thorup, 2003](#)). In these cases link “distance” does not even exist for non-links.

We shall also show that techniques which depend on existence tests of all edges have time complexity $O(n^2)$, where n is the number of nodes in the graph, whereas our estimation method has time complexity $O(e)$, where e is the number of edges in the graph. This can result in a dramatic improvement in computation time as large real graphs are often very sparse.

Waxman graphs are an example of the general class of SERNs (Spatially Embedded Random Graphs) (Kosmidis et al., 2008). One aim of this work is to develop intuition which can be extended to estimation of the parameters of random graphs from the general class. We will leave consideration of the general case to later work because complex questions of existence and identifiability arise.

3. General properties of Waxman graphs

The starting point for the creation of a Waxman random graph is to generate a set of n points uniformly at random in some region R of a metric space Ω . For any given region we can derive a probability density function $g(t)$ for the distance between an arbitrary pair of random points. This is commonly called the Line-Picking-Problem: for instances of regions including lines, balls, spheres, cubes, and rectangles see Ghosh (1951); Rosenberg (2004) and Weisstein (c,b,e,d,a).

Given the distribution of distances between points, we can calculate the probability that an arbitrary link exists (prior to knowing the distances):

$$\mathbb{P}\{(i, j) \in \mathcal{E} \mid q, s\} = q \int_0^\infty \exp(-st)g(t) dt = q\tilde{G}(s), \quad (3)$$

for any $i \neq j$, where $\tilde{G}(s)$ is the Laplace transform of $g(t)$ (or equivalently it is the moment generating function w.r.t. to $-s$). We know that the Laplace transform at $s = 0$ of a probability density is the normalisation constraint, so $\tilde{G}(0) = 1$. Hence when $s = 0$ there is no distance dependence and the result is the GER random graph.

From this probability we can also compute features of the graph such as the average node degree

$$\bar{k} = (n - 1)q\tilde{G}(s), \quad (4)$$

from which we can derive values of q that produce given average degree for a given network size and s . From the handshake theorem we can derive the average number of edges to be

$$\bar{e} = n(n - 1)q\tilde{G}(s)/2. \quad (5)$$

We can then derive the distribution of the length d of a link in the Waxman graph, and we denote this by $f(d \mid q, s) = \mathbb{P}\{d_{ij} = d \mid (i, j) \in \mathcal{E}\}$ which is

$$\begin{aligned} f(d \mid q, s) &= \frac{\mathbb{P}\{(i, j) \in \mathcal{E} \mid d_{(i,j)} = d; q, s\} \mathbb{P}\{d_{ij} = d\}}{\mathbb{P}\{(i, j) \in \mathcal{E} \mid q, s\}} \\ &= \frac{g(d) \exp(-sd)}{\tilde{G}(s)}. \end{aligned} \quad (6)$$

Note the q is a thinning parameter, and thus should not change the link length distribution, and we can see that it vanishes from the distribution. Hence we generally write f omitting q , *i.e.*, $f(d | s)$.

The formula allows easy calculation of the mean length of links in the Waxman graph

$$\mathbb{E}[d | s] = \frac{1}{\tilde{G}(s)} \int_0^\infty t g(t) \exp(-st) dt = -\frac{\tilde{G}'(s)}{\tilde{G}(s)}. \quad (7)$$

For small distances t , region-boundary effects are minimal, and so the function $g(t)$ depends only on the dimension of the embedding space. For example the square and disk both have $g(t) \stackrel{t \downarrow 0}{\sim} 2\pi t$, which comes from the size of the ring of radius t . Given a Euclidean distance metric on a k -dimensional space the small t approximation is

$$g(t) \simeq \frac{k\pi^{k/2}}{\Gamma(k/2 + 1)} t^{k-1}, \quad (8)$$

which is the surface area of the $(k-1)$ -sphere (the surface of the hyper-sphere embedded in the k -dimensional Euclidean space).

Using the following theorem, we can derive large s approximations for the Laplace transforms of a Cumulative Density Function (CDF). We work here mainly with the probability density function $g(t)$, and this must be integrated to get the CDF, but otherwise the applicability should be clear.

THEOREM 1 ([FELLER \(1971\)](#), PP.445-6). *If $0 < a < \infty$, and we have a positive measure concentrated on $(0, \infty)$ defined by the CDF $H(t)$ with Laplace-Stieltjes transform $\tilde{H}(s)$, then*

$$H(t) \stackrel{t \rightarrow 0}{\sim} \frac{L(t)}{\Gamma(a+1)} t^a \Leftrightarrow \tilde{H}(s) \stackrel{s \rightarrow \infty}{\sim} L(1/t) t^{-a}, \quad (9)$$

where $L(t)$ is a slowly varying function at 0, where this is defined as a function where $\lim_{t \rightarrow 0} L(xt)/L(t) = 1$ for all $x > 0$.

Applying [1](#) for a k -dimensional Euclidean space we get

$$\tilde{G}(s) \stackrel{s \rightarrow \infty}{\sim} \frac{\pi^{k/2} \Gamma(k+1)}{\Gamma(k/2 + 1)} s^{-k}, \quad (10)$$

$$\tilde{G}'(s) \stackrel{s \rightarrow \infty}{\sim} \frac{-k\pi^{k/2} \Gamma(k+1)}{\Gamma(k/2 + 1)} s^{-k-1}, \quad (11)$$

$$\mathbb{E}[d | s] \stackrel{s \rightarrow \infty}{\sim} k/s. \quad (12)$$

The Waxman graph is usually defined in terms of a number of nodes and two parameters (q, s) . However, the critical feature relating these two is the node density on the space ρ . This parameter determines the number of nodes within a certain distance of a given node. [Davis et al. \(2014\)](#) showed the crucial importance of the relationship between density and the spatial deterrence function. We can see from the small t , large s approximations that this relationship is (absent of boundary effects) a simple inverse relationship that generalises to arbitrary dimension. Intuitively it arises because for

large s only short links are likely, and hence the boundaries of the region play little part in the distribution.

As a measure of the difference between the Waxman and GER link-distance distribution we use the Kullback-Leibler Divergence (KLD) ¶, which provides an Information Theoretic measure of the difference.

The KLD of distribution $f(t|s)$ from $g(t)$ is defined by

$$KLD(g(t)\|f(t|s)) = \int_0^\infty g(t) \ln \frac{g(t)}{f(t|s)} dt. \quad (13)$$

From (6) we can derive

$$\begin{aligned} KLD(g(t)\|f(t|s)) &= \int_0^\infty g(t) [\ln g(t) - \ln f(t|s)] dt \\ &= \int_0^\infty g(t) [\ln g(t) - \ln g(t) + st + \ln \tilde{G}(s)] dt \\ &= s \int_0^\infty tg(t) dt + \ln \tilde{G}(s) \int_0^\infty g(t) dt \\ &= s\mathbb{E}[d] + \ln \tilde{G}(s). \end{aligned} \quad (14)$$

Taking the small t , large s approximations we can see that

$$\begin{aligned} KLD(g(t)\|f(t|s)) &\stackrel{s \rightarrow \infty}{\sim} k + \frac{k}{2} \ln \pi + \ln \Gamma(k+1) - \ln \Gamma(k/2+1) - k \ln s \\ &\stackrel{s \rightarrow \infty}{\sim} c(k) - k \ln s. \end{aligned}$$

That is, the deviation for large s of the length distribution of the Waxman graph from the GER graph is a constant dependent on the dimension of the space minus a term proportional to the log of s .

The likelihood function for a particular Waxman graph under the usual independence assumption, given the lengths of the observed links \mathbf{d} , is

$$\mathcal{L}(s | \mathbf{d}) = \prod_{(i,j) \in \mathcal{E}} f(d_{i,j} | s). \quad (15)$$

We apply (15) below, even though links in the Waxman graph are only conditionally and not truly independent given the distances. This can be intuited by considering triangles (edges connecting sets of three nodes). The fact that the underlying distances are a metric forces the three distances to satisfy the triangle inequality and thus the three must be correlated. Fortunately the correlation is largely local. For instance, if we consider two distinct node pairs (i_1, j_1) and (i_2, j_2) , then the existence of edges (i_1, j_1) and (i_2, j_2) is independent (given no extra information). Thus correlations are largely mediated through common nodes. As a result we should expect weaker correlations as the number of nodes n grows (given a fixed number of edges) and similarly we expect the correlations to increase as the average node degree increases. We demonstrate how this affects various estimators below.

¶The KLD is not strictly a distance metric because it lacks symmetry, hence the term “divergence”.

4. Estimation Techniques

This section describes various approaches to the parameter estimation of Waxman random graphs.

4.1. Log-linear regression

The first estimation method applied to this problem was introduced by [Lakhina et al. \(2002\)](#). They noted that

$$\frac{f(d | s)}{g(d)} = c \exp(-sd), \quad (16)$$

where we can see from our calculations that $c = 1/\tilde{G}$. If we could form this ratio, we might estimate s by log-linear regression against d . The observed lengths of links in the graph yield implicit measurement of the numerator in (16) and we could obtain estimates of $g(d)$ either:

- (a) *analytically*: use the shape of the region to compute $g(d)$; or
- (b) *empirically*: use the distances between all of the nodes (not just the linked nodes) to estimate $g(d)$.

The former has the advantage of being fast. The latter exploits the data itself in the case that the region is not regular, but computationally it is $O(n^2)$. The latter approach was used by [Lakhina et al. \(2002\)](#), but we shall evaluate both.

We also need to estimate $f(d | s)$: [Lakhina et al. \(2002\)](#) did so by forming a histogram. We shall use this approach, so the estimator proceeds by counting the number of edges in each length bin, and dividing by the expected number in that bin absent the distance deterrence function.

Once we have computed \hat{s} , we estimate q by inverting (5) to get

$$\hat{q} = \frac{2e}{n(n-1)\tilde{G}(\hat{s})}, \quad (17)$$

where n and e are the observed number of nodes and edges respectively. The decoupling of estimation of s and q makes this sequential estimation possible, and this will be exploited in other estimators described below.

The time complexity of the above algorithm based on the analytical formulation of $g(d)$ is $O(e)$ but if we were to estimate $g(d)$ using the distances between all nodes then it would be $O(n^2)$. Our evaluation focuses on the time to perform the regression, *i.e.*, we do not include the time to construct the distances and empirical histograms as these are problem dependent. For instance, Euclidean distance calculations are fast, but in one case we compute distances on the globe (including corrections for its non-spherical nature) and these calculations can be considerably slower.

4.2. Generalised Linear Model (GLM)

[Davis et al. \(2014\)](#) use a GLM to estimate the parameters of their model, ours is slightly different. In order to make the difference in usage explicit we include a description of

the framework taken from (Casella and Berger, 2002, p. 591). A GLM consists of three components:

A random component: The response variables Y_1, Y_2, \dots, Y_n . These are assumed to be independent (but not identically distributed) random variables from a specified exponential family.

A systematic component: a linear function of a vector of predictor variables

$$\beta_0 + \sum_{m=1}^k \beta_m \mathbf{X}^{(m)}, \quad (18)$$

where $\mathbf{X}^{(m)}$ is the m th predictor variable.

A link function: $r(\mu)$ such that

$$r(\mu_i) = \beta_0 + \sum_{m=1}^k \beta_m \mathbf{X}_i^{(m)}, \quad (19)$$

where $\mu_i = \mathbb{E}[Y_i]$, and \mathbf{X}_i is the predictor vector for the i th response.

Estimation of the β_m is usually by maximum likelihood, *i.e.*, we write the log likelihood, differentiate with respect to β_m and set to zero, giving $k + 1$ non-linear equations which are solved numerically. Here we use Matlab's `glmfit` to perform the task.

We index the variables by their edge label (i, j) and the response variables $Y_{(i,j)}$ are indicators of edges so \mathbf{Y} is the adjacency matrix of the graph, *i.e.*,

$$Y_{(i,j)} = \begin{cases} 1, & \text{if } (i, j) \in \mathcal{E}, \\ 0, & \text{otherwise.} \end{cases} \quad (20)$$

These are modelled as Bernoulli random variables, and hence $\mu_{(i,j)} = p(d_{i,j})$, *i.e.*, the probability that edge exists given that the distance between nodes i and j is $d_{i,j}$. The predictors are the distances, *i.e.*, $X_{(i,j)} = d_{i,j}$ and $k = 1$.

The probabilities are assumed to follow (1), so the natural link function is log. In this case we get

$$\log(p_{(i,j)}) = \beta_0 + \beta_1 d_{i,j}, \quad (21)$$

and make the natural identification that $\beta_0 = \log(q)$ and $\beta_1 = -s$.

The GLM of Davis et al. (2014) is almost identical but for the use of the link function $r(p_{(i,j)}) = \log(-\log(1 - p_{(i,j)}))$.

When the response random variables are Bernoulli, it is more conventional to use a logit link function. The advantage of this is that it maps the entire range of linear combinations of the systematic component into the interval $(0, 1)$, and thus produces legitimate probabilities.

Using log as the link function for modelling Waxman graphs means there is an implicit bound on the parameters β_m such that $\beta_0 + \beta_1 d_{i,j}$ must be positive. As long as the estimator returns positive parameters, this is assured, but in cases such as small s it is

possible to have examples where natural estimates lie on the boundary. Similar issues arise for our estimator, so we defer further discussion until section 4.5.

One potential problem with fitting a GLM is that if there is a cutoff c such that for all $d_{ij} \leq c$ the edge exists and for all $d_{ij} > c$ the edge is absent, then the GLM may not find finite coefficients that best fit the data and estimates will have large errors. This is unlikely to happen when estimating the parameters of large networks since the probability as a function of d decays exponentially, so there is no clean cutoff. However, in small networks there may only be a few edges, and it is possible that the data exhibit such a cutoff by chance. In cases with $n \sim 10$ we observe very poor performance for GLM fits as a result of this phenomena, but it has negligible impact on the accuracy of GLM fits for larger networks.

The GLM method uses all possible edges: those that exists and those that do not. Hence the number of response variables in the problem is $O(n^2)$, and so the computational time complexity is also $O(n^2)$.

4.3. Sufficient Statistics

An obvious question arises as to what is a set of *minimal sufficient statistics* for use in the estimation of Waxman random graph parameters. To answer this we apply the following theorem:

THEOREM 2 (CASELLA AND BERGER (2002), THEOREM 6.2.13, P.281).

Let $f(\mathbf{x} | \theta)$ be the PMF or PDF of a sample \mathbf{X} . Suppose there exists a function $T(\mathbf{x})$ such that, for every two sample points \mathbf{x} and \mathbf{y} , the ratio $f(\mathbf{x} | \theta)/f(\mathbf{y} | \theta)$ is a constant function of θ if and only if $T(\mathbf{x}) = T(\mathbf{y})$. Then $T(\mathbf{X})$ is a minimal sufficient statistic for θ .

Take the sample to be the set of edge lengths $\mathbf{d} = (d_1, \dots, d_e)$ where $d_k = d_{(i,j)}$ for $(i, j) \in \mathcal{E}$. Under the independence assumption the PDF of a sample is $\prod_{i=1}^e f(d_i | s, q)$, conditional on the number of edges e , where f is defined in (6), and e is binomially distributed $B_p^N(e)$ where $N = n(n-1)/2$ and $p = q\tilde{G}(s)$.

Consider two samples: $\mathbf{x} = (x_1, \dots, x_{e_1})$ and $\mathbf{y} = (y_1, \dots, y_{e_2})$, then the ratio in 2 is

$$\begin{aligned} \frac{B_p^N(e_1) \prod_{i=1}^{e_1} f(x_i | s, q)}{B_p^N(e_2) \prod_{i=1}^{e_2} f(y_i | s, q)} &= \frac{B_p^N(e_1) \prod_{i=1}^{e_1} g(x_i) e^{-sx_i} / \tilde{G}(s)}{B_p^N(e_2) \prod_{i=1}^{e_2} g(y_i) e^{-sy_i} / \tilde{G}(s)} \\ &= \frac{\prod_{i=1}^{e_1} g(x_i)}{\prod_{i=1}^{e_2} g(y_i)} \times \frac{\prod_{i=1}^{e_1} e^{-sx_i}}{\prod_{i=1}^{e_2} e^{-sy_i}} \times \frac{\tilde{G}(s)^{e_2} B_p^N(e_1)}{\tilde{G}(s)^{e_1} B_p^N(e_2)} \\ &= m(\mathbf{x}, \mathbf{y}) e^{-s(e_1 \bar{d}_x - e_2 \bar{d}_y)} \tilde{G}(s)^{e_2 - e_1} \frac{B_p^N(e_1)}{B_p^N(e_2)}, \end{aligned} \quad (22)$$

where \bar{d}_x and \bar{d}_y are the averages of the distances in datasets \mathbf{x} and \mathbf{y} respectively, and $m(\mathbf{x}, \mathbf{y})$ is a function only of $g(\cdot)$ of \mathbf{x} and \mathbf{y} , independent of the parameters (q, s) .

The ratio above depends on the parameters s and q only through the statistics \bar{d} and e . Hence if $e_1 = e_2$ and $\bar{d}_x = \bar{d}_y$, the ratio is a constant function of (q, s) . On the other hand, if either $e_1 \neq e_2$ or $\bar{d}_x \neq \bar{d}_y$, then the ratio is a non-constant function of the

parameters. Hence the conditions of the theorem are satisfied and (e, \bar{d}) forms a minimal sufficient set of statistics. Notably, these statistics can be constructed almost trivially in $O(e)$ time, and we will use that fact to construct a MLE.

4.4. Maximum Likelihood Estimator

We consider the log-likelihood function $\ell(s \mid \mathbf{d}) = \ln \mathcal{L}(s \mid \mathbf{d})$ and note from (15) that

$$\begin{aligned} \ell(s \mid \mathbf{d}) &= \sum_{(i,j) \in \mathcal{E}} \ln f(d_{(i,j)} \mid s) \\ &= \sum_{(i,j) \in \mathcal{E}} \left[\ln g(d_{(i,j)}) - s d_{(i,j)} - \ln \tilde{G}(s) \right] \\ &= -e \ln \tilde{G}(s) + \sum_{(i,j) \in \mathcal{E}} \ln g(d_{(i,j)}) - s \sum_{(i,j) \in \mathcal{E}} d_{(i,j)}. \end{aligned}$$

Our goal is to find s such that the partial derivative of $\ell(s \mid \mathbf{d})$ w.r.t. s is zero, *i.e.*,

$$\frac{\partial}{\partial s} \ell(s \mid \mathbf{d}) = -e \frac{\tilde{G}'(s)}{\tilde{G}(s)} - \sum_{(i,j) \in \mathcal{E}} d_{(i,j)} = 0, \quad (23)$$

so we need to find s such that

$$\frac{\tilde{G}'(s)}{\tilde{G}(s)} = -\frac{1}{e} \sum_{(i,j) \in \mathcal{E}} d_{(i,j)} = -\bar{d}, \quad (24)$$

where \bar{d} is the observed mean link length.

From (7) we know $-\tilde{G}'/\tilde{G}$ is the expected length of line segments on the Waxman graph, so the MLE of s is also the moment-matching estimator.

4.5. Existence and uniqueness of the MLE

When will a unique solution to (24) exist? We know from the definitions of $\tilde{G}(s)$ and its derivative that $\tilde{G}(s) > 0$, and $h(s) = -\tilde{G}'(s)/\tilde{G}(s)$ is a continuous, positive function for all s , so if $h(\cdot)$ is monotonic there will be at most one solution to (24) for any given \bar{d} .

Consider the derivative

$$\frac{dh}{ds} = \frac{\tilde{G}'(s)^2 - \tilde{G}''(s)\tilde{G}(s)}{\tilde{G}(s)^2}. \quad (25)$$

Now the numerator is positive, and from Schwarz's Inequality

$$\begin{aligned} \tilde{G}''(s)\tilde{G}(s) &= \int \left| \sqrt{t^2 g(t)} e^{-st} \right|^2 dt \cdot \int \left| \sqrt{g(t)} e^{-st} \right|^2 dt \\ &> \left| \int t g(t) e^{-st} dt \right|^2 \\ &= \tilde{G}'(s)^2, \end{aligned}$$

and so the denominator is negative, and hence the function $h(s)$ is monotonically decreasing with s .

When $s = 0$, the Laplace transform $\tilde{G}(0) = 1$ and hence $h(0) = \int tg(t)dt = \bar{g}$, the average distance between pairs of nodes. When we remove longer links preferentially, the average link distance must decrease, so it is intuitive that $h(s)$ is a decreasing function, starting at $h(0) = \bar{g} = d_{max}$, which is the maximum expected edge distance over all possible parameters s .

In the limit as $s \rightarrow \infty$ we already know from (12) that $h(s) = \mathbb{E}[d] \sim k/s$, and so we know that in the limit as $s \rightarrow \infty$ that $h(s) \rightarrow 0$, so for any measured $\bar{d} \in (0, d_{max}]$ there will be a unique solution to (24).

Unfortunately, it is possible for the sample mean of the edge distances $\bar{d} > d_{max}$, *i.e.*, for a particular graph to have an unlikely preponderance of longer links. In this case (24) has no solution for $s \in [0, \infty)$, which seems to create problems. However, the obvious interpretation of $\bar{d} > d_{max}$ is that then there is no evidence that long links have been preferentially filtered from the graph, and so it is natural in this case to assume the model should be the GER random graph, *i.e.*, $s = 0$.

In formal terms, the MLE satisfies some but not all of the properties required for it to be *consistent*. Standard asymptotic theory for MLEs requires the condition that the true parameter value lies away from the boundary to form consistent estimates that converge to the true value as the amount of data increases.

For more formal consideration of this boundary case, we could introduce a strict hypothesis test for GER vs Waxman graphs, but for the moment we take $s = 0$ in these cases. We will see that in these cases that this leads to a slight bias in estimates for graphs with small s . The bias leads to a variance-bias tradeoff, leading to a RMS error in the estimator that can be lower than the Cramér-Rao (CR) bound (for unbiased estimators).

In the case where the parameter s does lie away from the boundary, ideal MLEs have a number of useful properties:

- *Consistency*: a sequence of MLEs converges in probability to the value being estimated as the amount of data increase: in particular the estimates are asymptotically unbiased.
- *Efficiency*: *i.e.*, it achieves the CR lower bound when the sample size tends to ∞ , *i.e.*, no consistent estimator has lower asymptotic mean squared error.

Another way to state these results is that MLEs are *asymptotically normal*, *i.e.*, as the sample size increases, the distribution of the MLE tends to the Gaussian distribution with mean given by the true parameter, and covariance matrix equal to the inverse of the Fisher information matrix.

However, we know that our MLE does have a potential problem at the boundary, and that the independence assumption is an approximation, and so it is interesting to consider whether the ideal bound is actually achieved. In the next section we derive the CR lower bound against which we make comparisons.

4.6. Bounds

The CR lower bound is the minimum variance of any unbiased estimator, under certain mild conditions. In the case of a scalar parameter such as s , the bound is given by the inverse of the Fisher information $I(s)$ defined by

$$I(s) = -\mathbb{E}\left[\left(\frac{\partial^2 \ell(d; s)}{\partial s^2}\right)\right]. \quad (26)$$

Here we have already computed the first derivative of the likelihood in (23), and its second derivative is

$$\frac{\partial^2 \ell}{\partial s^2} = e \frac{dh}{ds}, \quad (27)$$

where we calculated dh/ds in (25). Taking the expected value, and noting (5), we get

$$I(s) = \frac{n(n-1)q}{2} \left[\frac{\tilde{G}''(s)\tilde{G}(s) - \tilde{G}'(s)^2}{\tilde{G}(s)^2} \right]. \quad (28)$$

The net effect of this result is that an estimator that achieves the CR bound would have variance $O(1/n^2)$.

However, that assumes that growth of the number of edges is $O(n^2)$, but a more reasonable model might increase the size of the network while keeping the average node degree \bar{k} constant, in which case (4) implies that the variance will be $O(1/n)$. Examples of this can be seen in the results.

Even if the network is not sparse, if we randomly sample $O(n)$ edges, then the result above implied that the variance will be $O(1/n)$, with the benefit that (for some estimators) the cost of computation will now be $O(n)$.

The mean squared error of an estimator is composed of the variance plus the bias-squared, so it is possible for a biased estimator to improve on the bound (as we shall see in special cases below), but in general we measure estimator efficiency (with respect to accuracy as a function of the amount of data) with respect to this bound.

4.7. MLE of \hat{q}

As noted above, once we know \hat{s} , we can use this to estimate \hat{q} using (17). If we know the exact value of s then q acts as a random filter of links, so estimation of q is equivalent to estimating the parameter of a Bernoulli process. Thus (17) would be the MLE of q given the true value of s . The question is whether it is still a MLE when we derive it from the estimated value of \hat{s} .

To answer this question we draw on the property of functional invariance of MLE *i.e.*, if parameters are related through a transformation $a = g(s)$, then the MLE of a is $\hat{a} = g(\hat{s})$. This property allows the conversion back to the original Waxman parameter $\alpha = 1/sL$, for instance. More importantly it means that $\hat{q} = 2e/n(n-1)\tilde{G}(\hat{s})$ is the MLE of q , given a MLE of \hat{s} .

Once again, the property above applies for the ideal MLE. We test the estimator \hat{q} , and we show that its properties are close to those of the ideal MLE, except when s is small.

4.8. Numerical calculation of the MLE

MLEs are often computed directly using techniques such as Newton’s method. In this problem, each iteration would require computation of a Laplace transform^{||}, and its derivative, and so will be somewhat slower than many MLEs. However, we can improve this performance in several ways. First, we rearrange (24) in the form

$$\bar{d}\tilde{G}(s) + \tilde{G}'(s) = \mathcal{LT}[(\bar{d} - t)g(t); s] = 0, \quad (29)$$

which reduces the number of transforms that need to be calculated.

The estimation algorithm is a 1D search using Matlab’s `fzero` function. No doubt faster implementations are possible using Newton-Raphson or other approaches, but we found this to converge in only a few steps, given reasonable starting bounds, which we choose to be $[0, k/\bar{d}]$ (where the upper bound is given by the asymptotic form of the average distance (12)).

In the particular case that $\bar{d} > d_{max}$, *i.e.*, the sample mean of the edge distances is greater than the largest expected edge distance, then we take $\hat{s} = 0$.

The speed of calculation can be improved if we precalculate $g(t)$ at a set of fixed grid points, and reuse this in all of the Laplace transform calculations, thus avoiding frequent recomputation of the density. We create a second estimate, the MLE-N (Numerical), in which we calculate the inverse CDF at uniformly spaced probabilities to minimise errors arising from the fixed grid. In the test below we use a grid of 1000 points. We will see that this approach allows faster computation at the cost of a small increase in error for large s . The tradeoff could be adjusted by adapting the number of points used.

The other reason for using points spaced uniformly in the probability space is that it is relatively easy to estimate an inverse CDF from data. In particular we could, if available, take the complete set of distances between all nodes and derive from this an empirical estimate of the inverse CDF to use in the MLE calculations. We refer to this method as the MLE-E (Empirical). This method avoids the problem of estimating the region size and shape, and the assumption that nodes are uniformly distributed over the space.

5. Tests

In this section we examine the performance of the Waxman graph parameter estimators on simulated data. There are three key parameters for a Waxman graph, s , q and n . Instead of using these we choose s , n , and the average node degree \bar{k} which implicitly determine q . We primarily focus on fairly sparse networks ($\bar{k} = 3$) because sparsity is the common case for many real networks, but we do examine the effect of changes in these parameters (note there are some combinations of these parameters for which q cannot exist).

The accuracy of the methods increase as the graphs become larger so we choose parameter values that result in moderately sized (1000 node) graphs. This ensures that errors are of a magnitude that allows us to compare and assess them. However, we do also examine the relationship between graph size and accuracy of parameter estimates.

^{||}The Laplace transforms are calculated numerically using Matlab’s `integral` function, which performs adaptive numerical quadrature.

Except where otherwise noted we simulate 1000 Waxman random graphs for each parameter setting using Matlab, and form estimates of bias and RMS (Root-Mean-Square) error for each estimation method. All unannotated results are for the Waxman graph on the unit square with the Euclidean distance metric.

5.1. Comparisons

We start with a basic test of the estimation methods. We consider the RMS (Root Mean Squared) errors of the methods with respect to the CR lower bound as a function of the parameter s . [Figure 1](#) shows these errors. The most obvious conclusions are that the log-linear regression is the least accurate and that the GLM and MLE estimators are all roughly equivalent in accuracy. The minor empirical variants of the log-linear and MLE estimators apparently have only small effects on accuracy.

However, when we examine a more detailed view in [Figure 2](#) some differences are apparent. Over the entire range the GLM tracks the CR bound, but for small values of s there is some advantage in using the GLM and MLE-E. For very small s , the MLE approaches can actually beat the CR bound. This can be explained by the constraint $s \geq 0$. This constraint leads to a small bias in the MLE estimators for small s . When s is around 1, the bias leads to an increase in the RMS errors. When s is very small the estimators have slightly more information than assumed in our naive CR bound, and this can reduce the variance of the estimator ([Gorman and Hero, 1990](#)).

For large values of s the MLE-E and MLE-N show a small increase in error compared to the exact MLE, because for large s the grid size chosen is not small enough for accurate integrals to be calculated. This effect could be mitigated by choosing a finer grid or by choosing a non-uniform grid with more detail around $t = 0$ (albeit at additional computational cost). We will leave the adaption of grid size to future work.

For small to moderate values of s , the MLE-E estimator is slightly better than its exact cousin. This is valuable, but remember that the MLE-E requires the information on all distances, not just those of the existing edges, whereas the MLE and MLE-N estimators need only the measurement of \bar{d} . In fact for large graphs the \bar{d} used the exact MLE could be calculated from a sample of edges, so it is possible to achieve sub- $O(e)$ performance for such graphs. We have examined a number of parameter settings and have observed the same trends in the results and below we examine accuracy as a function of other parameter values.

The major source of error can be seen in [Figure 3](#), which shows the bias in the various approaches. We see immediately that the log-linear approach suffers from significant bias which increases with s and remains the major source of error in the method. The GLM is almost unbiased except for very small networks, where the technique breaks down completely, resulting in very large errors. On the other hand, we see that the MLE is almost unbiased even for small networks, except for small s where there is a small positive bias that explains the increase in RMS errors in that domain.

We also estimate computation times using Matlab's *tic/toc* timers to estimate wall-clock time of execution, and take the median over our 1000 samples to provide a robust estimate of the typical computation times. Compute times are shown in [Figure 4](#), where we can see that the GLM takes quadratic time. The log-linear-E method (not shown) is also quadratic, but with a much smaller constant than the GLM, because a histogram

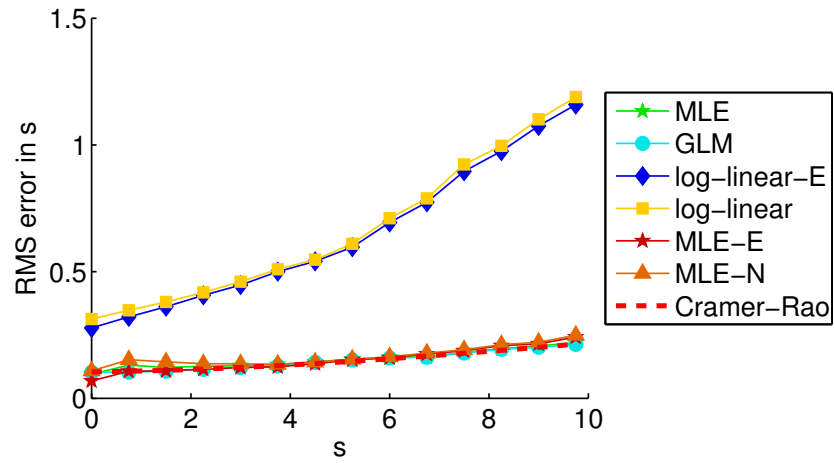


Fig. 1. RMS errors as a function of s ($\bar{k} = 3, n = 1000$). See [Figure 2](#) for detail.

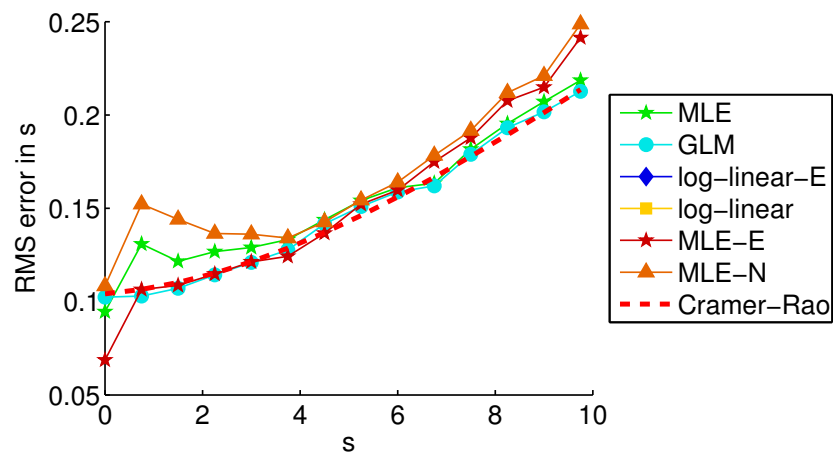


Fig. 2. RMS errors as a function of s ($\bar{k} = 3, n = 1000$) detail.

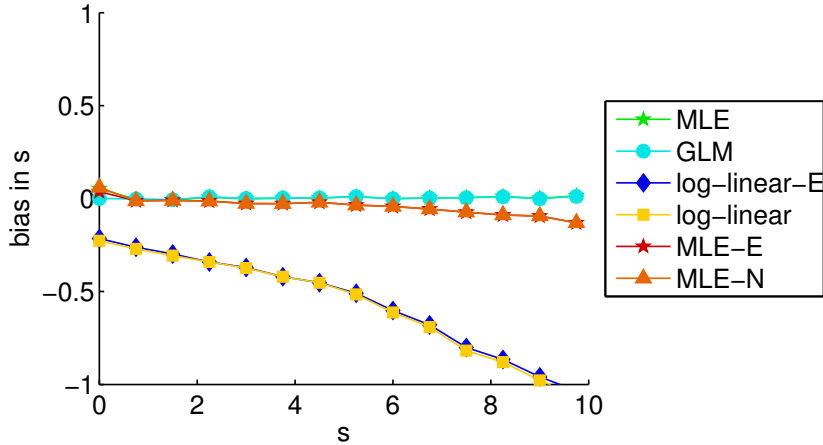


Fig. 3. Bias in \hat{s} for the different methods ($\bar{k} = 3, n = 1000$).

must be formed from all of the distances.

The other methods appear to have constant time with respect to the network size n . Constant time is an illusion however: these methods are actually $O(e)$, which for the networks considered is also $O(n)$. The constant time component is obviously dominant for the network sizes considered – we would expect to see the linearity only if we examine very large networks.

Memory requirement for the algorithms are

- GLM: $O(n^2)$;
- log-linear (and -E variant): $O(b)$ where b is the number of histogram bins;
- MLE: $O(1)$ (assuming the numerical quadrature is memory efficient); and
- MLE-E and MLE-N: $O(c)$ where c is the number of grid points.

Note that all but the GLM use constant memory as a function of network size, as they are based on summary statistics that can be computed via a streaming algorithm that does not need to hold data in memory.

There is little doubt that if accuracy is the prime consideration then the GLM is the best approach, whereas if there is a need for speed we can trade off a small amount of accuracy, and use the MLE or MLE-E. However, the practical considerations mean the GLM is not viable for large networks. Extrapolating the computation times for the GLM shown in Figure 4, we can see that computation would take in the order of 100 seconds for a graph of 10,000 nodes (and 15,000 links), or around 3 hours for a graph with 100,000 nodes. Similarly the GLM requires a large amount of memory for larger networks, as compared with the almost trivial amount required in the other algorithms. On the other hand, the accuracy of the log-linear approaches is poor. Consequently we shall consider only the MLE-based estimates in detail in what follows.

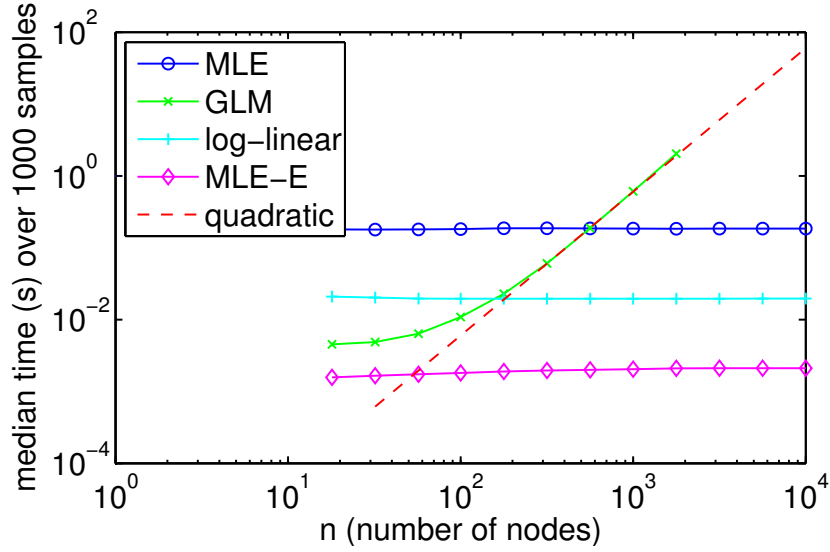


Fig. 4. Computation times ($s = 4$, $\bar{k} = 3$). Note that only the estimator time is included, not the time to form the matrix of distances needed in the GLM and log-linear methods.

5.2. MLE in detail

We now consider the accuracy of the MLE as both a function of the network size n in Figure 5(a) and of the average node degree \bar{k} in Figure 5(b). The accuracy of the method is close to the CR bound for all parameter ranges, but suffers slightly for small networks n , and for higher average node degree.

All of the previous results consider accuracy of parameter estimates of the Waxman graph over the unit square. Our approach naturally extends to a variety of scales, regions, and distance metrics. Figure 6(a) shows the CR bounds for estimator accuracy as a function of the length of the side of the square region, and Figure 6(b) shows these bounds for different region shapes.

In the first case estimator accuracy is worse in smaller regions. In such regions, all points are compacted closer together, and there is a smaller range of possible length scales. Thus we must estimate the exponential decay factor over a smaller range of scales. The effect is more dramatic for smaller s values, where longer links are still likely. As $s \rightarrow \infty$ the CR bounds converge because the length scale of typical links drops well below the lengths of typical (potential) links.

In the second case there are variations between regions but most have the same rough shape as a function of s . Notable exceptions are sphere and hyper-sphere which are not monotonically increasing functions of s as the others are.

It is also notable that all of the methods have the same asymptotic slope for large s (though the function for the hyper-sphere is truncated because larger s is invalid given the fixed values of n and \bar{k} used in this plot). The overall conclusion is that the shape of the region does have an effect (up to almost a factor of 2 in estimator accuracy at some parameter values). However, the the shape of the region is not the most important factor

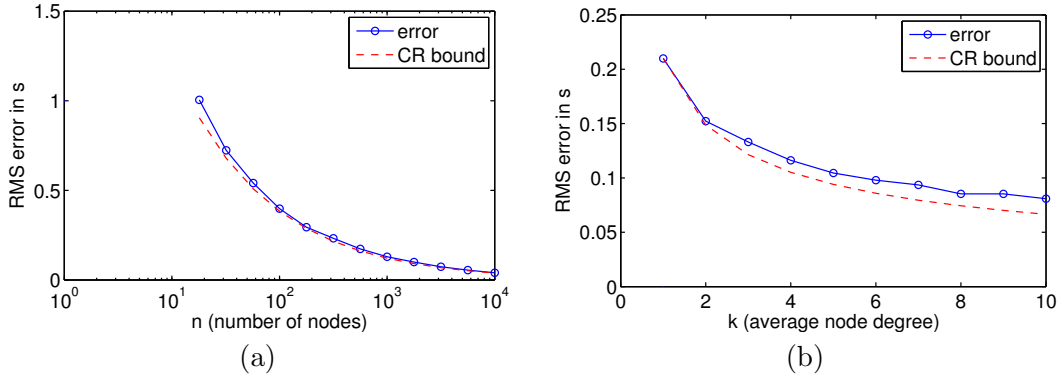


Fig. 5. Accuracy of the MLE as a function of other parameters of the network (default parameters $n = 1000$, $s = 3.0$, and $\bar{k} = 3$)

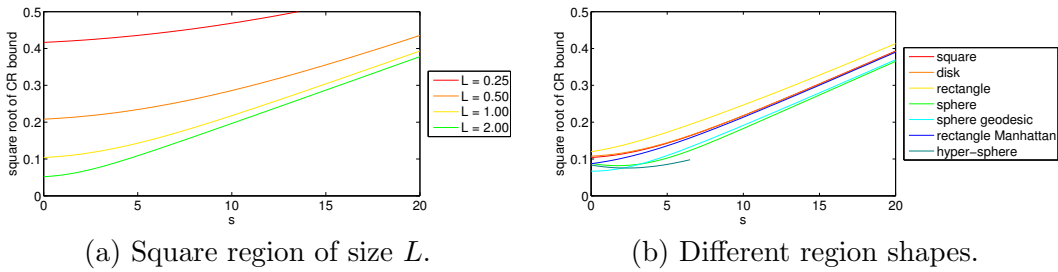


Fig. 6. CR bounds for different regions.

in determining the accuracy of the estimator: the size of the graph, and its parameters play a larger role.

5.3. Robustness

More importantly, it is possible that we will not know the exact shape of the region of interest, or that the shape used in estimation is an approximation of an irregular region. In these cases we could use the empirical estimates of the potential links, but if the shape of the region is unknown, it is important to consider the impact of an erroneous decision. Figure 7 shows that impact by highlighting the relative size of the induced error as a result of assuming the wrong shaped region for three different region shapes (a square, a disk and a rectangle with an aspect ratio of 2:1).

Figure 7(a) shows that there is a certain robustness, as choosing the disk instead of the square or visa versa leads to only a small increase in error. On the other hand, assuming a square or disk when the region is really a rectangle causes much larger errors. The difference is that the longer thinner rectangle has a considerably larger boundary to area proportion, and the boundary effects play a larger role in the random line distribution.

Comparison of Figure 7(a) and (b) suggests that the effect is more significant for smaller values of s . This is because larger values of s result in shorter links on average

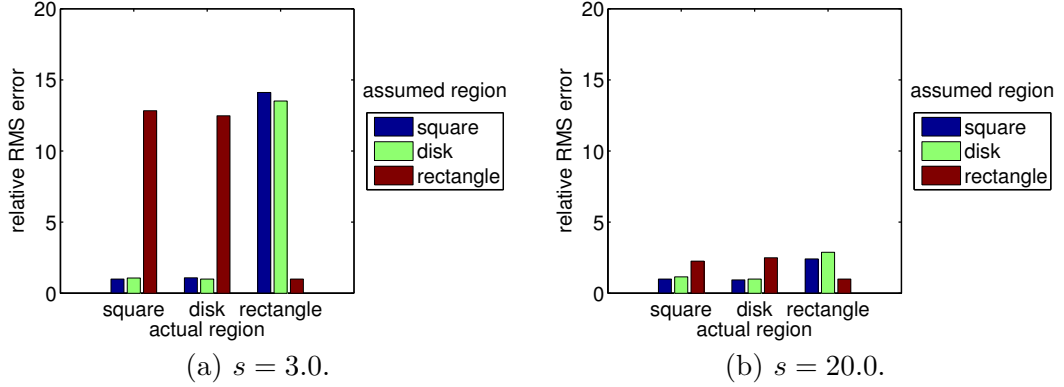


Fig. 7. Relative RMS error when the assumed region shape is incorrect. Note that errors are much smaller for large s values, because boundary effects play a lesser role.

hence boundary effects play a smaller role. So unsurprisingly, the estimates are more robust for large s .

We also consider the impact of estimating the size of the region. Figure 8 shows RMS errors for a disk-shaped region when the diameter is known (Real), when it is estimated by taking the largest link-distance (Est 1), and when it is estimated using the largest inter-node distance (Est 2).

The loss in estimator accuracy when the size of the region is unknown is clear. Further, the inaccuracy increases with s because as s increase, the longest observed link is less likely to be a proxy for the actual size of the region. We could correct for this bias, but instead we compare to estimates of the region size formed from the maximum inter-node distance, and we see that there is almost no loss of accuracy in the estimator.

The conclusion is that some knowledge of the region over which the graph is drawn is important. Very poor estimates of the region can result in much worse estimator accuracy, but there is a fair amount of robustness so the estimate of the region shape and scale need not be perfect and estimates drawn from the data are sufficient.

Finally, to test how robust the model outputs are when the underlying model is incorrect, *i.e.*, the distance deterrence function is not Waxman, we test the performance of the MLE when the underlying graph is actually the DASTB model (Davis et al., 2014) used for the vole contact graph data. We use this model as a comparison, because it is very similar in concept, but has different details. Figure 9 shows that there is some very small induced bias in the estimates as a result of applying the model in the wrong situation, but these would have almost no influence on the conclusions drawn from \hat{s} estimates.

5.4. Estimating \hat{q}

In most of the preceding work we have only considered the accuracy of the estimates for s . The estimated accuracy of q is that of the binomial model parameter estimate which is well understood except for the manner in which errors in \hat{s} propagate into the

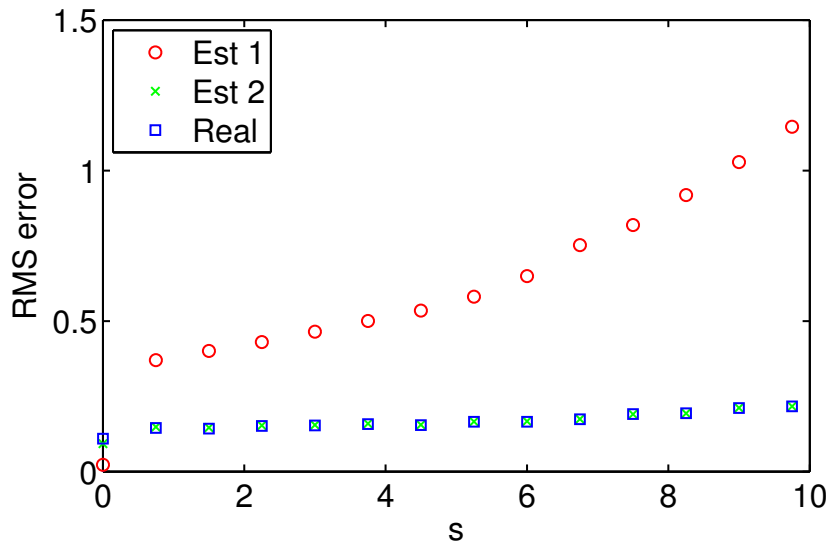


Fig. 8. The impact of estimating the size of the region. Real is the MLE given the real region size. Est 1 is the MLE given the region size is estimated using the longest link, and Est 2 is the MLE given the region size is estimated from the longest inter-node distance. We see that estimating the region size using the inter-node distances introduced minimal errors, but using the link distances increases the errors, except for very small s .

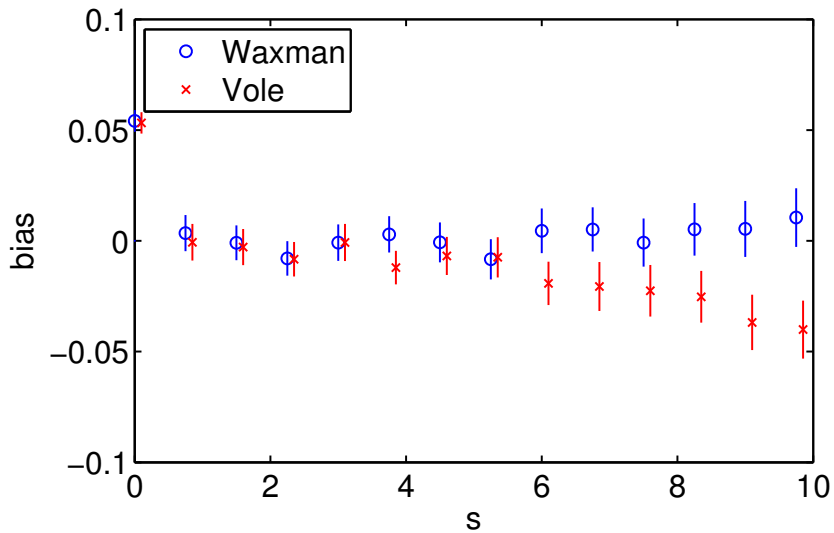


Fig. 9. Estimates \hat{s} when the underlying network is not Waxman, but rather drawn from the DASTB vole-contact model. For smaller s , using the wrong model introduces minimal addition error.

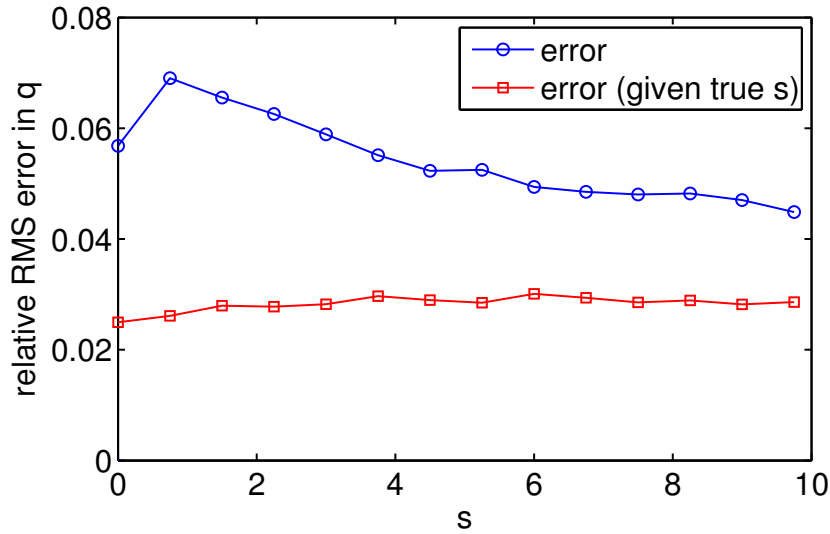


Fig. 10. Relative error for the MLE \hat{q} ($n = 1000$, $\bar{k} = 3$). Squares indicate the RMS error relative to q assuming we were given the true s values, and circles indicate the error of the actual estimator.

estimate \hat{q} through $\tilde{G}(\hat{s})$.

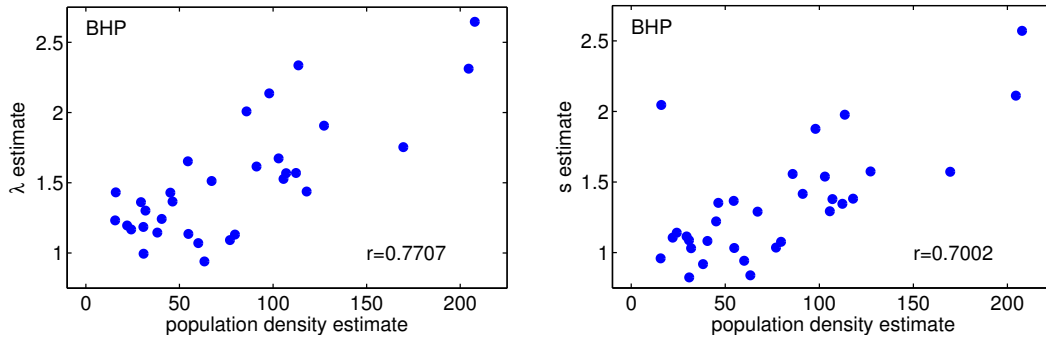
Figure 10 shows the RMS errors in \hat{q} relative to the size of q , given the estimated and true values of s . We can see from the figure that the errors in \hat{q} are roughly doubled by the uncertainty in \hat{s} , so this error does have a significant effect. However, the errors in \hat{q} are still small: *i.e.*, of the order of 4%.

6. Case studies

The previous section looked at accuracy on simulated data, where we know the ground truth. This section considers how well the method works on real data. We consider three datasets, one biological and two Internet.

6.1. Vole data

Davis et al. (2014) collected a large mark-recapture dataset on the English–Scottish border over a 7-year period to study relationships between field voles (*Microtus agrestis*). In particular, they considered a number of models for the contact graphs created by relationships between the voles. A grid of trap locations was created on each of four sites and over 64 capture periods traps were emptied multiple times. Contact graphs were built by associating voles that were caught in the same trap on separate occasions. In their main dataset, the time periods were divided into pairs and each pair used to construct one graph, so in total 32 graphs were created for each site. One might argue with the methodological accuracy of constructing contact graphs from trap data in this manner, but there is no doubt that this is an unusually large dataset of related graphs. It



(a) Reproduction of Figure 5(a) from (Davis et al., 2014).

(b) Equivalent plot of \hat{s} estimates against population density.

Fig. 11. Vole data: data drawn from the Black Blake Hope (BHP) site: r reports the correlation coefficients.

is rare to have more than a few example contact graphs in any one application. The large number of these graphs allows some views of estimates that are not usually available.

Davis et al. (2014) fitted multiple models to the data including a GER random graph, and their DASTB model, which resembles the Waxman graph. Their model incorporated the capture process as an explicit component and they form an edge in the graph when one or more contacts occurred.

Using the original raw data provided by the authors we reconstructed their contact graphs and confirmed we could reproduce the results obtained in (Davis et al., 2014). Estimates of λ (their distance parameter) were recomputed using the complimentary log-log regression to confirm that the recreated graphs and their measured statistics were correct, and that the units were correct. Figure 11(a) reproduces Davis et al. (2014, Figure 5(a)), demonstrating that the data has been correctly reconstructed.

Next we performed our own estimates using the MLE with the underlying region being a square of side 10 (comprised of 10 traps with a 5m spread between each, thus matching the experiment. Figure 11(b) shows our estimates (we have repeated the same procedure for all four original datasets with similar results). We can see from the graph that although estimates of s are not the same as λ , the general conclusion of (Davis et al., 2014) that there is a correlation between population density and the spatial contact parameter is supported with almost the same correlation coefficient being reported for both datasets.

The results emphasise the original findings of Davis *et al.*, notably that:

- Animal contact graphs are well modelled by spatial graphs (in our case there is a small difference in the particular model, but the general behaviour is similar).
- This modelling provides a means of quantifying differences between two groups of animals (separated in time or space).
- The parameter \hat{s} tells us something important that other many models omit, namely that the distance voles travel when contacting each other decreases with population

Table 1. Summary of Mercator datasets: number of nodes, edges, and the average link distance.

Region	n	e	\bar{d} (miles)
USA	123426	152602	384.7
EUROPE	32928	30049	319.5
JAPAN	14318	16665	317.6

density. Thus has a profound importance for disease transmission (Davis et al., 2014) in that population mixing may not increase with population density as quickly as is often assumed.

More generally, models can be used for the usual suite of purposes such as simulation and extrapolation. For example, once we know the length scale at which contact is unlikely, we might use this in the design of capture/recapture experiments by choosing the scale and resolution of the capture setup.

6.2. Internet dataset 1

Lakhina et al. (2002) undertook one of the first attempts to formally quantify the exponential decrease of link likelihood as a function of distance. The authors compared two sets of data and found consistent results between them. They provided one of these datasets (the Mercator data) to us for comparison. Lakhina *et al.* separated the data into three regions, and analysed these separately. Table 1 provides a brief summary of the three regions.

We do not argue that this network is random in any real sense: in fact the Internet networks are the result of design. However, fitting a Waxman-like graph to these is instructive in that it shows how engineering constraints lead to distance-sensitive link placement.

We can see first from the data that the graphs are large but very sparse, with average node degrees of around 2. In this dataset we also have node locations so we can derive distances between all pairs of nodes and thus apply all of the possible techniques considered here. However, it is not feasible to use the GLM approach for this scale of problem.

Lakhina et al. (2002) applied log-linear regression to the question. We applied the MLE and compared the results to those found in their work. Table 2 provides a comparison between various estimates, including the original values reported in Lakhina et al. (2002) given in the second column under $\hat{s}_{Lakhina}$. Units are *per 1000 miles* — we use Imperial units to be consistent with the original paper. The third column provides our equivalent estimate. There are small differences, presumably because of differences in the exact numerical procedures applied.

The fourth column of the table shows the MLE-E values estimated for the datasets. We use the Empirical estimator because the region shapes are irregular (*e.g.*, the USA), and we want to avoid approximation errors arising from the region shape.

We see considerable discrepancies which are larger than can be explained by errors

Table 2. Estimates: $\hat{s}_{Lakhina}$ are the values from [Lakhina et al. \(2002\)](#); and $\hat{s}_{log-linear}$ are our corresponding estimates. Units are *per 1000 miles*. The \hat{s}_{MLE-E} values are derived from our Empirical MLE, and the \hat{s}_{MLE-T} values from a version of the MLE with distance data truncated in the same manner as the original log-linear estimates.

Region	$\hat{s}_{Lakhina}$	$\hat{s}_{log-linear}$	\hat{s}_{MLE-E}	\hat{s}_{MLE-T}
USA	6.91	6.38	2.75	6.63
EUROPE	12.80	12.81	30.92	10.09
JAPAN	6.89	6.71	45.91	7.30

in the log-linear regression approach. However, reading [Lakhina et al. \(2002\)](#), we can see that their estimates are over a truncated range of distances for two reasons:

- The node locations they use are artificially quantised by the Geolocation procedure so some nodes appear to have exactly the same position, and hence zero distance, when actually there is a positive distance between the nodes; and
- They found that the exponential distance-deterrence function fit the data only up to some threshold distance.

In their (and our comparison) log-linear regressions the range over which we perform the regression is restricted to be between these bounds.

In order to provide a fair comparison we also modified the MLE-E by censoring the potential edges used in forming the CDF and in computing the average edges distance. [Table 2](#) shows the results under s_{MLE-T} to be closer to being consistent with the log-linear regression.

The results point to one valuable feature of the log-linear regression, which is that it comes with diagnostics. Examination of the fit indicates whether the model is appropriate or not. The MLE requires additional effort to provide similar diagnostics. On the other hand, there are significant issues with the log-linear regression. Apart from being less accurate, there is the question of bin size which simple experiments seem to suggest has more effect on estimates than one might hope.

Ultimately, all of the methods suggest strongly that a spatial component should be part of any model for Internet linkages. This is entirely consistent with the intuition of engineers who work on such networks: long links cost more, and so are rarer.

6.3. Internet dataset 2

Finally we apply the MLE to a set of real networks from the Internet Topology Zoo ([Knight et al., 2011](#)). The networks – taken at Point of Presence (PoP) level – show the connectivity of a sample of seven major network operators in different regions of the world. [Figure 12](#) shows one example, and the seven are summarised and results shown in [Table 3](#).

These graphs are much smaller as a result of being drawn at the PoP level, and so errors in the estimates will be correspondingly larger. However, there is a very clear variation in the parameters.

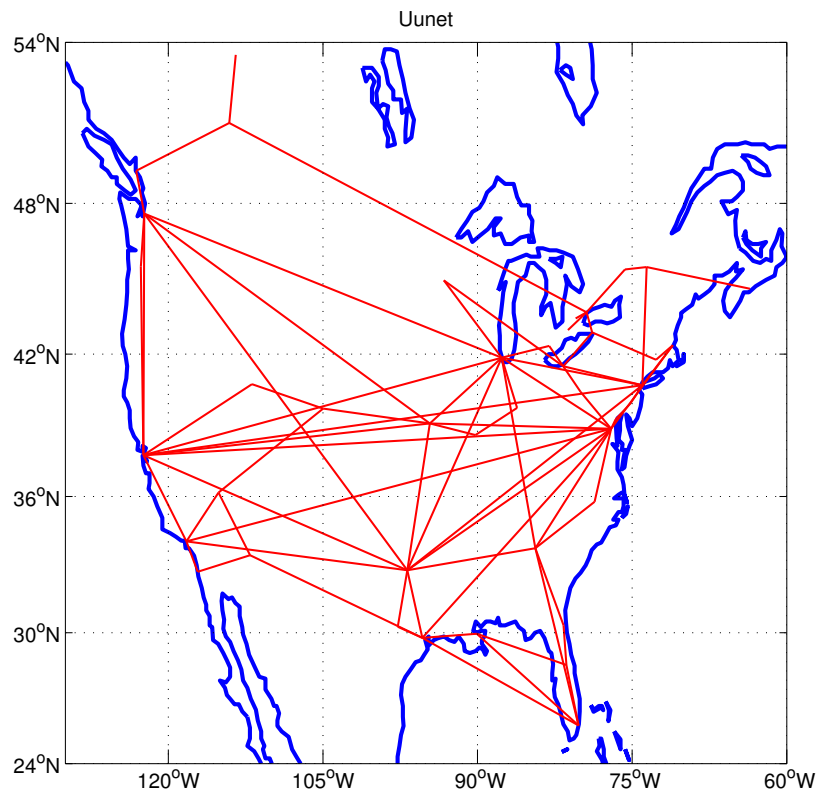


Fig. 12. The UUNET network from the Internet Topology Zoo.

Table 3. Estimates for Internet Topology Zoo data. Units for s are per 1000 km.

Network	Region	n	e	\bar{d}	\hat{s}_{MLE-E}
Aarnet	Australia	19	24	695.6	2.20
Iinet	Australia	9	12	1472.9	0.30
BtEurope	Europe	22	35	606.3	2.05
Colt	Europe	153	177	160.2	9.48
Abilene	USA	11	14	1007.0	1.39
Internetmci	USA	19	33	927.7	1.25
Uninet	USA	42	77	966.9	1.09

Firstly, although the units for s here are per 1000 km, we can clearly see that the s estimates are a good deal smaller than for the previous dataset, largely because of looking at a single network at a time, at the PoP level. Router-level networks (such as the previous dataset) include numerous routers, many of them connected, in the same cities. The interconnects between networks also tend to be shorter as they are mediated through Internet exchange points or carrier hotels. However, at the PoP level, all of these small-scale details are invisible, and consequently we see less strong distance deterrence.

Secondly, we see a wide variety of s values, with little relationship to region. Networks are just different. They are built with different goals, and different cost structures and constraints. Some are new, and others are older and incorporate legacy components.

The wide variety of network structures has been observed in the Zoo data before (Bowden et al., 2014), but not with respect to spatial structure. This reinforces the message that estimates of model parameters such as s provide alternative methods to compare network behaviour.

7. Discussion and Conclusion

This paper presents the MLE for the parameters of the Waxman graph and demonstrates its accuracy in comparison to alternative estimators. The MLE has two advantages. Firstly it can guarantee $O(n)$ computational time complexity and constant memory usage by using only a sample of the edges that exist in a graph to estimate s . Secondly it can be applied in domains where the coordinates of nodes are unknown and/or edge lengths may be weights in some arbitrary process. Using the MLE we have shown that real networks have a considerably wider range of s parameters than is typically used in the literature.

The next question might be: “Is the Waxman model a better model than X?” where X might be the GER random graph, or some other model. Davis et al. (2014) considered this question using AIC, but for the simple question of testing whether there should be a distance term or not, it is perhaps more natural to use a hypothesis test. We applied the standard likelihood ratio test and found that standard threshold choices resulted in poor ability to specify the significance. It seems the problem arises from the failure of the independence assumption. If so the problem is correctable, but we leave the question of correctly determining the cutoff threshold for future work.

8. Acknowledgements

We would like to thank [Davis et al. \(2014\)](#) for providing us with their vole data, and [Lakhina et al. \(2002\)](#) for providing the first Internet dataset. The Zoo data is publicly available at www.topology-zoo.org.

This work was supported by the Australian Research Council through grant DP110103505, and the Centre of Excellence for Mathematical & Statistical Frontiers.

References

- Ahuja, S. S., Ramasubramanian, S. and Krunz, M. M. (2009) Single-link failure detection in all-optical networks using monitoring cycles and paths. *IEEE/ACM Transactions on Networking*, **17**, 1080–1093.
- Bowden, R., Roughan, M. and Bean, N. (2014) Cold: PoP-level topology synthesis. In *CoNext*. Sydney, Australia.
- Carzaniga, A., Rutherford, M. J. and Wolf, A. L. (2004) A routing scheme for content-based networking. In *IEEE INFOCOM*.
- Casella, G. and Berger, R. L. (2002) *Statistical Inference*. United States: Thomson Learning, 2 edn.
- Costa, L. D. F., Rodrigues, F. and Boas, P. V. (2010) Modeling the evolution of complex networks through the path-star transformation and optimal multicariate methods. *International Journal of Bifurcation and Chaos*, **20**, 795–804.
- Davis, S., Abbasi, B., Shah, S., Telfer, S. and Begon, M. (2014) Spatial analyses of wildlife contact networks. *Journal of The Royal Society Interface*, **12**. <http://rsif.royalsocietypublishing.org/content/12/102/20141004.short>.
- Doar, M. and Leslie, I. (1993) How bad is naive multicast routing? In *IEEE INFOCOM*, 82–89. San Francisco, CA, USA.
- Erdős, P. and Rényi, A. (1960) On the evolution of random graphs. *Publications of the Mathematical Institute of the Hungarian Academy of Sciences*, **5**, 17–61.
- Fang, Y., Chu, F., Mammarr, S. and Che., A. (2011a) Iterative algorithm for lane reservation problem on transportation network. In *Networking, Sensing and Control (ICNSC), 2011 IEEE International Conference on*, 305–310.
- Fang, Y., Mammarr, S., Chu, F. and Che, A. (2011b) The capacitated lane reservation problem in transportation network. In *Logistics (LOGISTIQUA), 2011 4th International Conference on*, 439–444.
- Feller, W. (1971) *An Introduction to Probability Theory and its Applications*, vol. II. John Wiley and Sons, New York, second edn.
- Fortz, B. and Thorup, M. (2003) Robust optimization of OSPF/IS-IS weights. In *Proc. INOC 2003* (eds. W. Ben-Ameur and A. Petrowski), 225–230.
- (2004) Increasing Internet capacity using local search. *Computational Optimization and Applications*, **29**, 13–48. Online: <http://dx.doi.org/10.1023/B:COAP.0000039487.35027.02>.

- Ghosh, B. (1951) Random distance within a rectangle and between two rectangles. *Bulletin of the Calcutta Mathematical Society*, **43**, 17–24.
- Gilbert, E. (1959) Random graphs. *Annals of Mathematical Statistics*, **30**, 1441–1444.
- Gorman, J. D. and Hero, A. O. (1990) Lower bounds for parametric estimation with constraints. *IEEE Transactions on Information Theory*, **36**, 1285–1301.
- Gunduz, C., Yener, B. and Gultekin, S. H. (2004) The cell graphs of cancer. *Bioinformatics*, **20**, 145–151.
- Guo, L. and Matta, I. (2003) Search space reduction in QoS routing. *Computer Networks*, **41**, 73–88.
- Holzer, M., Schulz, F., Wagner, D. and Willhalm, T. (2005) Combining speed-up techniques for shortest-path computations. *J. Exp. Algorithmics*, **10**, 2.5.
- Huang, L., Han, H. and Hou, J. (2007) Multicast routing based on the ant system. *Applied Mathematical Sciences*, **1**, 2827–2838.
- Janssen, J. (2010) Spatial models for virtual networks. *Lecture Notes in Computer Science*, **6158/2010**, 201–210.
- Kaiser, M. and Hilgetag, C. C. (2004a) Modelling the development of cortical systems networks. *Neurocomputing*, **58-60**, 297–302. Online: <http://www.sciencedirect.com/science/article/pii/S0925231204000554>. Computational Neuroscience: Trends in Research 2004.
- (2004b) Spatial growth of real-world networks. *Phys. Rev. E*, **69**. Online: <http://pre.aps.org/abstract/PRE/v69/i3/e036103>.
- Knight, S., Nguyen, H., Falkner, N., Bowden, R. and Roughan, M. (2011) The Internet topology zoo. *IEEE Journal on Selected Areas in Communications (JSAC)*, **29**, 1765–1775.
- Kosmidis, K., Havlin, S. and Bunde, A. (2008) Structural properties of spatially embedded networks. *Europhysics Letters*, **82**. Online: <http://iopscience.iop.org/0295-5075/82/4/48005>.
- Kuipers, F. A. (2004) *Quality of Service Routing in the Internet: Theory, Complexity and Algorithms*. Ph.D. thesis, Technische Universiteit Delft.
- Lakhina, A., Byers, J. W., Crovella, M. and Matta, I. (2002) On the geographic location of Internet resources. In *ACM SIGCOMM Workshop on Internet Measurement (IMW)*, 249–250. New York, NY, USA: ACM. Online: <http://doi.acm.org/10.1145/637201.637240>.
- Lua, E. K., Griffin, T., Pias, M., Zheng, H. and Crowcroft, J. (2005) On the accuracy of embeddings for Internet coordinate systems. In *ACM Sigcomm MC*.
- Malladi, S., Prasad, S. and Navathe, S. (2007) Improving secure communication policy agreements by building coalitions. In *Parallel and Distributed Processing Symposium, 2007. IPDPS 2007. IEEE International*, 1–8.
- Matta, I. and Guo, L. (1999) QDMR: an efficient QoS dependent multicast routing algorithm. In *Proceeding of 5th IEEE realtime technology and application symposium (RTAS '99)*.
- M.Naldi (2005) Connectivity of Waxman graphs. *Computer Communications*, **29**, 24–31.

- Neve, H. D. and Mieghem, P. V. (2000) TAMCRA: a tunable accuracy multiple constraints routing algorithm. *Computer Networks*, **23**, 667–679.
- Rastogi, R., Silberschatz, A. and Yener, B. (2001) Algorithms for provisioning virtual private networks in the hose model. In *IEEE/ACM Transactions on Networking*, 135–146.
- Rosenberg, E. (2004) The expected length of a random line segment in a rectangle. *Operations Research Letters*, **32**, 99–102. Online: <http://www.sciencedirect.com/science/article/pii/S0167637703000725>.
- Salama, H. F., Reeves, D. S. and Viniotis, Y. (1997) Evaluation of multicast routing algorithms for real-time communication on high-speed networks. *IEEE Journal on Selected Areas in Communications*, **15**, 332–345.
- Shaikh, A., Rexford, J. and Shin, K. G. (1999) Load-sensitive routing of long-lived IP flows. In *ACM Sigcomm*.
- Thomas, M. and Zegura, E. W. (1994) Generation and analysis of random graphs to model internetworks. *Tech. Rep. GIT-CC-94-46*, Georgia Institute of Technology. <http://smartech.gatech.edu/handle/1853/6735>.
- Tran, D. A. and Pham, C. (2009) PUB-2-SUB: a content-based publish/subscribe framework for cooperative P2P networks. In *Networking 2009: 8th International IFIP-TC 6 Networking Conference*, 770–781.
- Van Mieghem, P. (2001) Paths in the simple random graph and the Waxman graph. *Probab. Eng. Inf. Sci.*, **15**, 535–555. Online: <http://dl.acm.org/citation.cfm?id=982639.982646>.
- Verma, S., Pankaj, R. K. and Leon-Garcia, A. (1998) QoS based multicast routing algorithms for real time applications. *Performance Evaluation*, **34**, 273–294.
- Wang, J., Li, L., Low, S. H. and Doyle, J. C. (2005) Cross-layer optimization in TCP/IP networks. *IEEE/ACM Transactions on Networking*, **13**, 582–595.
- Waxman, B. (1988) Routing of multipoint connections. *IEEE J. Select. Areas Commun.*, **6**, 1617–1622.
- Wei, L. and Estrin, D. (1994) The trade-offs of multicast trees and algorithms. In *Proc. Int. Conf. Computer Communications and Networks (ICCCN'94)*, 902–926.
- Weisstein, E. W. (a) Ball line picking. From MathWorld—A Wolfram Web Resource. <http://mathworld.wolfram.com/BallLinePicking.html>.
- (b) Circle line picking. From MathWorld—A Wolfram Web Resource. <http://mathworld.wolfram.com/CircleLinePicking.html>.
- (c) Line line picking. From MathWorld—A Wolfram Web Resource. <http://mathworld.wolfram.com/LineLinePicking.html>.
- (d) Sphere line picking. From MathWorld—A Wolfram Web Resource. <http://mathworld.wolfram.com/SphereLinePicking.html>.
- (e) Square line picking. From MathWorld—A Wolfram Web Resource. <http://mathworld.wolfram.com/SquareLinePicking.html>.

- Wu, J.-J., Hwang, R.-H. and Lu, H.-I. (2000) Multicast routing with multiple QoS constraints in ATM networks. *Information Sciences*, **124**, 29–57. Online: <http://www.sciencedirect.com/science/article/pii/S0020025599001024>.
- Zegura, E. W., Calvert, K. and Bhattacharjee, S. (1996) How to model an internetwork. In *IEEE Infocom*, 594–602. San Francisco, CA.
- Zegura, E. W., Calvert, K. L. and Donahoo, M. J. (1997) A quantitative comparison of graph-based models for Internet topology. *IEEE/ACM Transactions on Networking*, **5**, 770–783.